Pediatr Radiol (2001) 31: 589–593

Ramiro J. Hernandez
Peter J. Strouse
Frank J. Londy
Thomas W. Wakefield

Gadolinium-enhanced MR angiography (Gd-MRA) of thoracic vasculature in an animal model using double-dose gadolinium and quiet breathing

Received: 7 November 2000
Accepted: 22 Feburary 2001

R. J. Hernandez (✉) · P. J. Strouse
Section of Pediatric Radiology,
University of Michigan Health System,
1500 E. Medical Center Drive,
Ann Arbor, MI 48109–0252, USA
e-mail rjhm@umich.edu
Tel.: + 1-734-763 2570
Fax: + 1-734-764 9351

F. J. Londy
Department of Radiology,
University of Michigan Hospitals,
Ann Arbor, MI 48109–0030, USA

T. W. Wakefield
Department of Surgery,
Section of Vascular Surgery,
University of Michigan Hospitals,
Ann Arbor, MI 48109–0329, USA

Abstract *Objective.* To evaluate a gadolinium-enhanced MR angiography (Gd-MRA) imaging protocol for the assessment of thoracic vessels using double-dose gadolinium and quiet breathing. An animal model was used to simulate imaging in infants and young children. *Material and methods.* Six baboons (*Papio anubis*), mean weight 5.7 kg, were sedated and intubated. After the injection of double-dose Gd-DTPA (0.2 mmol/kg) through a peripheral vein, a coronal spoiled 3D gradient-echo volume acquisition was obtained during quiet breathing. Two radiologists reviewed the images for visualization of aortic arch, brachiocephalic vessel origins, pulmonary arteries (central, upper lobe and descending branches), and pulmonary veins (upper and lower). *Results.* Visualization was excellent for the aortic arch, brachiocephalic vessel origins, and pulmonary arteries, including the hilar branches. Visualization was excellent for the lower and right upper pulmonary veins and fair for the left upper pulmonary vein. There was excellent agreement between radiologists. *Conclusion.* Imaging of thoracic vessels with Gd-MRA using double gadolinium during quiet breathing was effective in our animal model. The advantages of this technique include a short imaging time and depiction of vascular segments – branches of pulmonary arteries and intraparenchymal segments of pulmonary veins – not optimally visualized with other non-invasive imaging techniques.

Introduction

Since the introduction of 3D-gadolinium-enhanced MR angiography (3D-Gd MRA) by Prince [1], many reports have described the effectiveness of 3D-Gd MRA in the evaluation of the thoracic vessels [2–4]. Three dimensional-Gd MRA usually requires breath-holding and administration of high doses of gadolinium; therefore, the majority of subjects in these reports are adult patients. A recent report describes the use of a non-breath-hold Gd-3D-MRA in children using gadolinium doses ranging from 0.3 to 0.5 mmol/kg [5]. Besides using a high dose of gadolinium, this report did not address the feasibility of this technique in the visualization of thoracic vascular structures, such as the pulmonary arteries and veins.

The advantages of 3D-Gd MRA over other MR imaging techniques for the evaluation of the thoracic vessels include (1) rapid acquisition, (2) ability to image vessels in any plane, and (3) absence of dephasing artifact.

The purpose of this investigation was to evaluate a 3D-Gd MRA imaging protocol for the assessment of thoracic vessels in infants and young children using a double dose (0.2 mmol/kg body weight) of gadolinium and quiet breathing.

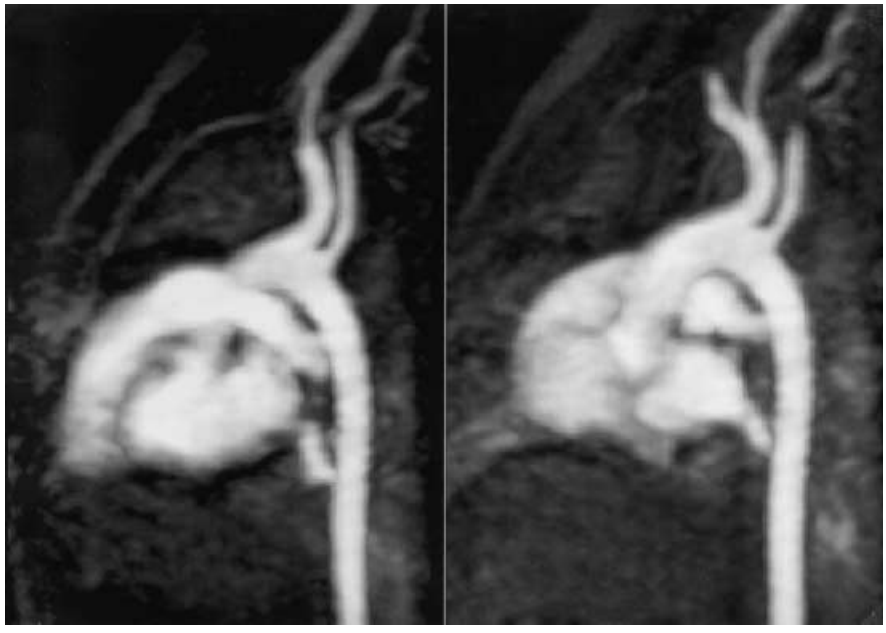

Fig. 1 Reformatted images [6/1.3 (repetition time-ms/echo time-ms), 30° flip angle] from a three-dimensional MR angiogram with gadopentetate dimeglumine enhancement. *Left* Sagittal reformatted image demonstrating the main pulmonary artery. *Right* Sagittal oblique reformatted image demonstrating the thoracic aorta and the origin of the two brachiocephalic vessel (baboons only have two brachiocephalic vessel)

Materials and methods

The University Committee on the Use and Care of Animals approved this protocol. An animal model was used to simulate the size of infants and young children. Six baboons (*Papio anubis*), approximately 2–3 years of age and mean weight of 5.7 kg, were sedated and intubated. The sedation protocol consisted of an injection of 1 cc of Telazol (Tiletamin HCl/Zolazepam HCl) at a dose of 10 mg/kg, I.M. and atropine sulfate 0.02 mg/kg 90 min before the study. Sedation was maintained with 0.6 cc boluses, as needed, of thiopental sodium 2.5% solution.

All baboons were imaged with a 1.5-T superconducting magnet (Signa; GE Medical Systems, Milwaukee, Wis.) with an anterior neck coil and software version 8.3. A sagittal T1-weighted spin-echo localizing sequence was obtained.

A coronal multiphase spoiled 3D dynamic gadolinium-enhanced fast spoiled gradient recalled-echo sequence was acquired during quiet breathing with the following imaging parameters: 6–6.1/1.3–1.5 (repetition time-ms/echo time-ms), 30° flip angle, 62.5 kHz bandwidth, frequency encoding superior to inferior, 20 × 14 cm field of view, a single excitation signal average acquired, 32 sections at 2.2 mm section thickness with 1.1 mm section separation via zero-fill interpolation, and a 256 × 160 matrix. Sequential κ-space filling was used. Five phases were obtained with the acquisition time being 22–24 s for each temporal phase and no pause between phases.

With approximately 4 s remaining in the first phase, 0.2 mmol/kg of body weight of gadopentetate dimeglumine (Gd-DTPA) (Magnevist; Berlex Laboratories, Wayne, N.J.) was hand-injected through a peripheral vein. No saline flush was used because the gadolinium was injected through an angiocath without intervening tubing.

Angiographic images were reconstructed using the Advantage Window Workstation (General Electric Medical Systems, Milwaukee, Wis.). Multiplanar volume reconstruction post-processing software was used as well as maximum intensity projections (MIP) and subvolume MIPs. Reformatted images were obtained in orthogonal and oblique planes to display the vessel of interest optimally.

Two radiologists independently reviewed the MIP images for visualization of aortic arch, brachiocephalic vessel origins, pulmonary arteries (central, upper lobe, and descending branches), and pulmonary veins (upper and lower). Structures were scored using a scale of: 0 = no visualization, that is, the vascular structure being evaluated could not be identified; 1 = fair visualization when the vascular structure being evaluated could be identified, but only partially; 2 = excellent visualization, that is, the vascular structure being evaluated was visualized in its entirety.

The Kappa statistic was used to evaluate the agreement between the two readers. Statistical significance was set at the 0.05 level. If the kappa statistic could not be calculated, due to the degree of agreement between observers and the small sample size, the agreement percentage, that is, the number of times that the observers agreed expressed as a percentage of total observations, was calculated.

Results

Visualization of the aortic arch, brachiocephalic vessel origins, pulmonary arteries, including the hilar branches, and the right upper and bilateral lower pulmonary veins was excellent (Figs. 1–4). Visualization of the left upper pulmonary veins was fair. Given the degree of agreement between observers and the small sample size, a kappa statistic could not be calculated in some instances. Therefore, the agreement percentage was calculated. There was excellent (kappa = 1) agreement between observers in classifying the visualization of the central pulmonary arteries, the branches of the right pulmonary artery, the right pulmonary veins, the aortic arch, and the origin of the brachiocephalic vessels. There was substantial (83.3%) agreement between observers in classifying the visualization of the left pulmo-

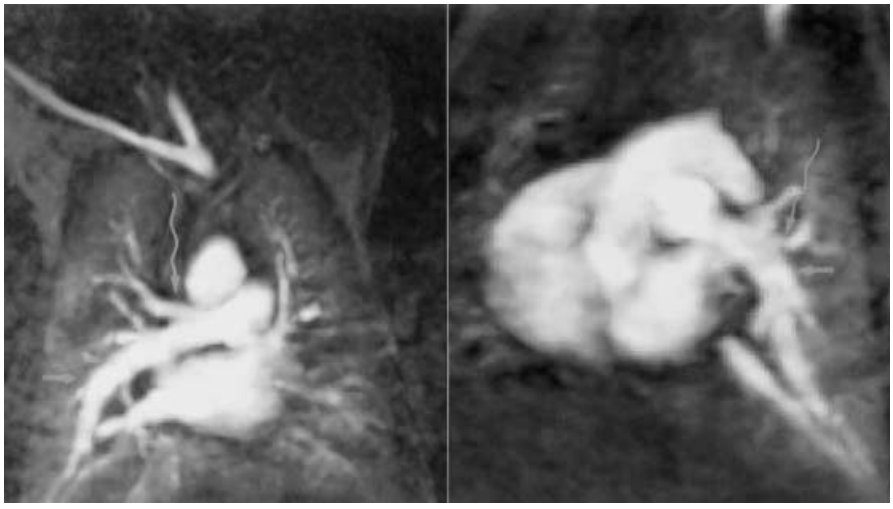

Fig. 2 Reformatted images [6/1.3 (repetition time-ms/echo time-ms), 30° flip angle] from a three-dimensional MR angiogram with gadopentetate dimeglumine enhancement. *Left* Coronal oblique reformatted image demonstrating the right pulmonary artery, right upper lobe branch (*long arrow*) and the descending branch of the right pulmonary artery (*short arrow*). *Right* Oblique sagittal reformatted image demonstrating the left upper lobe branch (*long arrow*) and the descending branch of the left pulmonary artery (*short arrow*)

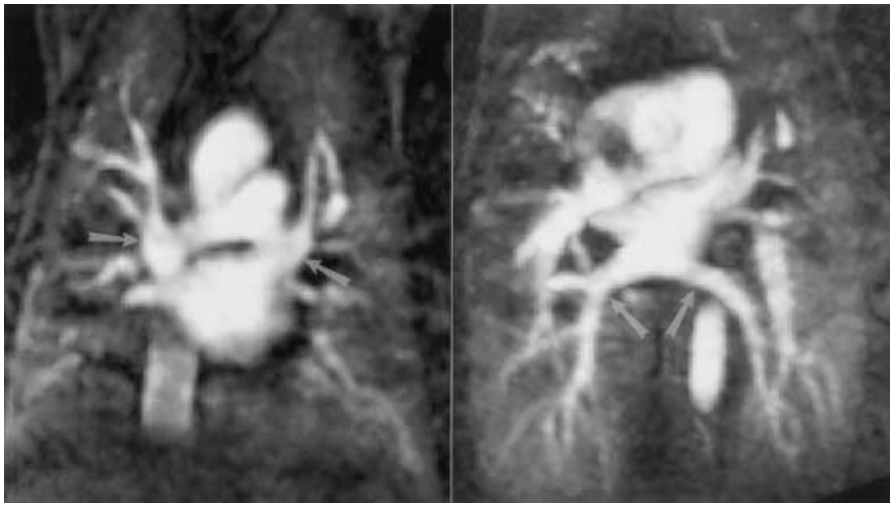

Fig. 3 Reformatted images [6/1.3 (repetition time-ms/echo time-ms), 30° flip angle] from a three-dimensional MR angiogram with gadopentetate dimeglumine enhancement. *Left* Coronal reformatted image demonstrating the upper lobe pulmonary veins (*arrows*). Note overlap of the right pulmonary artery with the right upper pulmonary vein. *Right* Coronal oblique reformatted image demonstrating the right and left lower pulmonary veins (*arrows*)

nary artery branches. There was significant disagreement (kappa = 0) between observers in classifying the visualization of the left upper pulmonary vein.

Discussion

In our animal model, 3D-Gd MRA using double-dose gadolinium (0.2 mmol/kg) and quiet breathing was effective in the evaluation of the aortic arch, brachiocephalic vessels, and pulmonary arteries and veins.

The morphologic assessment of the thoracic vessels in children with congenital heart lesions by MRI currently consists predominantly of T1-weighted cardiac gated spin-echo and segmented gradient-recalled echo sequences. Limitations of these techniques include inability to image vessels coursing on non-orthogonal planes, susceptibility to dephasing artifacts, and length of examination. Vascular segments such as the aortic arch and its branches, hilar regions of the pulmonary arteries including intraparenchymal branches, and pulmonary veins beyond the pericardial reflection are difficult to evaluate with T1-weighted cardiac gated spin-echo and segmented gradient-recalled echo sequences. The capability to reformat images in any plane with 3D-Gd MRA allows visualization of the aortic arch and its branches, the hilar regions including delineation of the upper lobe and descending branches of the pulmonary arteries, and the pulmonary veins beyond the pericardial reflection. Visualization of the upper pulmonary veins was less reliable because of partial obscuration by the overlying pulmonary arteries, despite various thickness multiplanar reconstructions.

A double dose of contrast was selected, since a double dose of gadolinium is effective in the evaluation of small vascular structures such as the segmental pulmo-

Fig. 4 Reformatted images [6/1.3 (repetition time-ms/echo time-ms), 30° flip angle] from a three-dimensional MR angiogram with gadopentetate dimeglumine enhancement. Coronal oblique reformatted image demonstrating the right and left lower pulmonary veins (*small arrows*). This view also provides excellent visualization of the right and left pulmonary arteries (*arrowheads*). The upper lobe branches of both pulmonary arteries can clearly be delineated (*long arrows*)

nary arteries in the adult [6]. Although there are studies documenting the effectiveness of lower doses in the adult [7–11], these studies usually were performed with breath-holding. In infants, the single dose (0.1 mmol/kg body weight) of contrast may be very small, i.e., a 7-kg patient will receive 1.4 cc of gadodiamide, which may make it difficult to administer as a bolus. Furthermore, data from the literature suggest there is no difference in adverse events between a lower and higher dose [12, 13]. Although in this study we used gadopentetate dimeglumine (Gd-DTPA), for children non-ionic contrast agents such as gadoteridol and gadodiamide may be desirable because of their lower osmolality and higher tolerance rates [14, 15].

Vascular visualization using Gd-enhanced 3D MRA relies on the T1 shortening of blood by gadolinium-chelate contrast media during its time of intravascular transit. The intravascular transit time of gadolinium in children is less predictable because of varying size of the patient, heart rate, and injection rate. Given the small amount of contrast able to be administered, estimation of the circulation time with pretest doses of contrast is not feasible. To circumvent the difficulty in predicting transit time we used a multiphase technique, thus ensuring that at least one of the temporal phases will have an optimal intravascular concentration of gadolinium. Although automatic trigger software techniques aimed at detecting the bolus of contrast in a specific vascular structure are frequently used, their utility in infants with congenital heart disease may be limited. Automatic trigger software techniques are designed to time breath-holding and the acquisition of central $\varkappa$-space to the arrival of contrast to a specific vascular structure. However, there are limitations to this technique. Breath-holding in infants requires intubation and general anesthesia, which should be avoided if possible. Secondly, small or absent vascular structures in patients with congenital cardiac lesions makes it difficult to standardize an optimal target volume for triggering from patient to patient. Finally, the presence of communications between vascular structures (i.e., ventricular septal defect, atrial septal defect, and surgical shunts) may dilute or alter the dynamics of the bolus.

Our imaging protocol takes advantage of strategies to decrease imaging time such as increasing bandwidth and acquiring only a portion of $\varkappa$-space (partial Fourier imaging) with zero-filling of the remaining lines. Although in our imaging protocol we did not take advantage of the centric phase encoding schemes (that acquire central lines of $\varkappa$-space at the beginning of the scan), this strategy may enhance the diagnostic quality of MRA by optimizing the calculation of delay time. However, a poorly timed centric acquisition can produce more severe artifacts than a sequential acquisition such as the one used in this research [16].

In our animal model, 3D-Gd MRA using a double dose of gadolinium and quiet breathing was an effective imaging technique in the evaluation of the thoracic vasculature. This technique allows optimal visualization of the aortic arch, the hilar branches of the pulmonary arteries, and the pulmonary veins that are difficult to evaluate with non-gadolinium MR imaging sequences or other imaging modalities. Given the size similarities between our animal model and infants or young children, this imaging protocol will be effective in the evaluation of the thoracic vasculature of infants or young children.

References

1. Prince MR (1994) Gadolinium-enhanced MR aortography. Radiology 191: 155–164
2. Hartnell GG, Finn JP, Zenni M, et al (1994) MR imaging of the thoracic aorta: comparison of spin-echo, angiographic and breath-hold techniques. Radiology 191: 697–704
3. Krinsky GA, Rofsky NM, DeCorato DR, et al (1997) Thoracic aorta: comparison of gadolinium-enhanced three-dimensional MR angiography with conventional MR imaging. Radiology 202: 183–193
4. Prince MR, Narasimham DL, Jacoby WT, et al (1996) Three-dimensional gadolinium-enhanced MR angiography of the thoracic aorta. AJR 166: 1387–1397
5. Lam WW, Chan JH, Hui Y, et al (1998) Non-breath-hold gadolinium-enhanced MR angiography of the thoracoabdominal aorta: experience in 18 children. AJR 170: 478–480
6. Hany TF, Schmidt M, Hilfiker PR, et al (1998) Optimization of contrast dosage for gadolinium-enhanced 3D MRA of the pulmonary and renal arteries. Magn Reson Imaging 16: 901–906
7. Lentschig MG, Reimer P, Rausch-Lentschig UL, et al (1998) Breath-hold gaolinium-enhanced MR angiography of the major vessels at 1.0 T: dose-response findings and angiographic correlation. Radiology 208: 353–357
8. Krinsky GA, Reuss PM, Lee VS, et al (1999) Thoracic aorta: comparison of single-dose breath-hold and double-dose non-breath-hold gadolinium-enhanced three-dimensional MR angiography. AJR 173: 145–150
9. Rofsky NM, Johnson G, Adelman MA, et al (1997) Peripheral vascular disease evaluated with reduced-dose gadolinium-enhanced MR angiography. Radiology 205: 163–169
10. Lee VS, Rofsky NM, Krinsky GA, et al (1999) Single-dose breath-hold gadolinium-enhanced three-dimensional MR angiography of the renal arteries. Radiology 211: 69–78
11. Earls JP, Rofsky NM, DeCorato DR, et al (1996) Breath-hold single-dose gadolinium-enhanced three-dimensional MR aortography: usefulness of a timing examination and MR power injector. Radiology 201: 705–710
12. Niendorf HP, Haustein J, Louton T, et al (1991) Safety and tolerance after intravenous administration of 0.3 mmol/kg Gd-DTPA. Results of a randomized, controlled clinical trial. Invest Radiol 26:S221–S223
13. Niendorf HP, Haustein J, Cornelius I, et al (1991) Safety of gadolinium-DTPA: extended clinical experience. Magn Reson Med 22: 222–228
14. Chang CA (1993) Magnetic resonance imaging contrast agents. Design and physicochemical properties of gadodiamide. Invest Radiol 28:S21–S27
15. Harpur ES, Worah D, Hals P-A, et al (1993) Preclinical safety assessment and pharmacokinetics of gadodiamide injection, a new magnetic resonance imaging contrast agent. Invest Radiol 28:S28–S43
16. Maki JH, Prince MR, Londy FJ, et al (1996) The effects of time varying intravascular signal intensity and κ-space acquisition order on three-dimensional MR angiography image quality. JMRI 6: 642–651